NASA TECHNICAL MEMORANDUM

NASA TM X-73687

NASA TM X-73687

THE DESIGN OF HYDRAULIC PRESSURE REGULATORS THAT ARE STABLE WITHOUT THE USE OF SENSING LINE RESTRICTORS OR FRICTIONAL DAMPERS

by Harold Gold
Lewis Research Center
Cleveland, Ohio 44135

TECHNICAL PAPER to be presented at the
National Conference on Fluid Power
sponsored by the Illinois Institute of Technology
Chicago, Illinois, October 25-27, 1977

THE DESIGN OF HYDRAULIC PRESSURE REGULATORS THAT ARE STABLE WITHOUT THE USE OF SENSING LINE RESTRICTORS OR FRICTIONAL DAMPERS

Harold Gold
Lewis Research Center

Prepared for National Conference on Fluid Power
Chicago, Oct. 1977

E-9220

Abstract

Parameters that are controlled in design determine the stability of hydraulic pressure regulators in service. The non-linear sensing line restrictor can provide stability, but degrades the transient response. Linear damping is not always physically realizeable and is sensitive to clearance and viscosity. Design relationships are analytically derived in this paper through which regulators can be made to be stable without the use of either of these damping means. The analytical distinctions between the parameters derived herein and those in the prior literature are discussed. An analytically derived circuit component that stabilizes an otherwise unstable regulator and its experimental verification is described.

Introduction

One of the most frequently occurring problems in hydraulic circuits is the elimination of pressure regulator instability. The regulator is usually the only active element, in the feedback sense, among the dynamically coupled hydraulic elements and stability is determined by the interaction of the regulator and the coupled passive elements of the circuit. Stability is a necessary but not sufficient condition for acceptable regulator performance and therefore, stabilizing means that cause an increase in response time or droop magnitude are not always acceptable. The analysis here reported presents a method by which stability margin, response and droop magnitude can be incorporated during design of direct acting hydraulic pressure regulators.

The sensing line orifice, which is frequently used for stabilization, imposes a very rapidly acting limit on the velocity of the variable orifice element of the regulator and thereby degrades response. Heavy mechanical damping of the variable orifice element can produce steady state error or cause limit cycle oscillation. When instability is the result of a high gain over the stability limit, the small line orifice or the large mechanical damping that is required to obtain stable operation may so severely restrict valve action that control effectiveness is lost. The design methods that are derived in this paper provide two means through which stability can be obtained in the complete absence of a line orifice or of mechanical damping.

The analysis is based on a generalized block diagram that represents the three elements: the pressure regulator, the flow or pressure generator and the coupled load. The coupled load is represented by its impedance. The diagram thereby yields the open loop transfer function of the system for any load whose circuit impedance can be expressed. The analysis is applied to the pump-supplied relief valve circuit, the load-supplied counter balance valve circuit, and the pressure-supplied reducing valve circuit. Relationships are provided for use in design to incorporate a specific gain margin for stability and for Bode diagram verification. Closed loop transfer functions are given from which the dynamic response of flow and pressure can be calculated from regulator design constant and circuit parameters.

The applicability to hydraulic circuits of the linear mathematical methods employed is well established, as presented in the cited literature which covers the span of the past twenty years. The list of references cannot be considered to be complete but it is believed to include those in major current use. The correspondence of the mathematical relationships that are derived herein with those given in the references is discussed at appropriate places in the paper. Electrical symbols are used in this paper to represent passive element flow or pressure coefficients. This use provides the reader with means to quickly identify the physical property being represented, a means which is not provided by the use of annomous, subscripted C's for coefficients of parameters of all physical properties.

Regulator Dynamics

Basic Circuit and Valve Configuration

A fundamental configuration of a pressure regulator of the relief type coupled to a positive displacement pump energized system is illustrated in figure 1.

The circuit load and the flow generator shown in the figure represent general impedances which will be treated in detail later. The valve element is a spring biased piston that operates in a sleeve, creating a variable orifice through the interaction of the piston with openings in the sleeve. The geometry illustrates a valve element which permits independent control, in design, of piston area and the lift to area gain of the variable orifice. This design controlability does not exist in poppet valve or full annulus spool valve configurations in which the ratio of piston area to the lift to area gain is fixed at one quarter of the piston diameter. Poppet and spool valves are in wide use and it is probably for this reason that most of the past literature (2-6) treats such valves; and as a further consequence, these references do not illustrate the strong effect of the area to gain ratio on stability. The analysis that follows treats piston area and variable orifice lift to area gain as independently selective parameters. In all other respects the derived relationships apply to all valve configurations.

Pressure and Flow Equations

In terms of the symbols defined in Appendix A, the flow through the variable orifice is

$$Q_V = DA_V\sqrt{P_R} \tag{1}$$

Considering perturbations about an equilibrium condition, the valve orifice area is

$$a_V = Wx_P \tag{2}$$

and equation (1) can be expressed by the linear equation

$$q_V = K_V x_P + \frac{1}{R_V} p_R \tag{3}$$

where

$$K_V = \left.\frac{\partial Q_V}{\partial X_P}\right|_{P_R} \qquad \text{and} \qquad R_V = 1\Big/\left.\frac{\partial Q_V}{\partial P_R}\right|_{X_P}$$

The partial derivatives are from equation (1)

$$K_V = DW\sqrt{P_R} \tag{4}$$

$$R_V = \frac{2P_R}{Q_V} \tag{5}$$

The flow equilibrium in the regulated pressure junction can be written

$$q_V + q_P + q_G + q_L = 0 \tag{6}$$

It is a mathematical convenience to write equation (6) with all the flow terms positive because, as will be seen below, the logic of direction is more apparent in consideration of the pressure gradients. Taking the flow direction into the junction positive and out negative, the flows to be substituted in equation (6) are

$$q_V = -K_V x_P - \frac{1}{R_V} p_R \tag{7}$$

$$q_P = -A_P S x_P \tag{8}$$

$$q_G = -\frac{1}{Z_G} p_R \tag{9}$$

$$q_L = -\frac{1}{Z_L} p_R \tag{10}$$

Substituting equations (7)-(10) in equation (6) and combining terms yields

$$p_R = -\frac{K_V(\tau_V S + 1)}{\left(\frac{1}{R_V} + \frac{1}{Z_G} + \frac{1}{Z_L}\right)} x_P \tag{11}$$

where

$$\tau_V = \frac{A_P}{K_V} \tag{12}$$

Force Equations

The forces that act on the piston result from pressure, spring deflection, viscous drag, piston inertia and the change of momentum of the flow discharging through the valve. The force equilibrium, in terms of perturbations can be written

$$f_P + f_S + f_I + f_D + f_Q = 0 \tag{13}$$

Taking the direction of force in the valve closing direction as positive, the forces are

$$f_P = -A_P(p_R - p_L) \tag{14}$$

$$f_S = K_{SP} x_P \tag{15}$$

$$f_I = M_P S^2 x_P \tag{16}$$

$$f_D = K_{DP} S x_P \tag{17}$$

$$f_Q = C_1 K_V x_P + \frac{2C_1}{R_V} p_R \qquad \text{(derived in App. B)} \tag{18}$$

Substituting equations (14)-(18) in equation (13) and combining terms yields

$$x_P = \frac{A_P[(1 - \alpha)p_R - p_L]}{M_P S^2 + K_{DP} S + K_{SP}(1 + \beta)} \tag{19}$$

where

$$\alpha = \frac{2C_1}{A_P R_V} \tag{20}$$

$$\beta = \frac{C_1 K_V}{K_{SP}} \tag{21}$$

Equation (19) can be written

$$x_P = \frac{\frac{A_P(1 - \alpha)}{K_S(1 + \beta)}\left[p_R - \frac{1}{(1 - \alpha)} p_L\right]}{\left(\frac{S^2}{\omega_P^2} + \frac{2\delta_P}{\omega_P} S + 1\right)} \tag{22}$$

where

$$\omega_P = \sqrt{\frac{K_{SP}(1 + \beta)}{M_P}} \tag{23}$$

$$\delta_P = \frac{K_{DP}}{2\sqrt{M_P K_{SP}(1 + \beta)}} \tag{24}$$

Equations (11) and (22) combined in block diagram form is shown in figure 2.

Relief Valve Pressure Regulator With A Parallel Capacitive Plus Resistive Load

In the relief valve circuits that are treated in the following sections the flow generator will be a positive displacement pump that runs at constant speed. The flow generator impedance will be represented by the leakage resistance of the pump.

The flow equilibrium in the impedance junction shown in figure 3 is

$$q_L + q_G + q_C + q_R = 0 \tag{25}$$

where

$$q_G = -\frac{1}{R_G} p_R \tag{26}$$

$$q_L = -C_L S p_R \tag{27}$$

$$q_R = -\frac{1}{R_L} p_R \tag{28}$$

Substituting equations (26)-(28) in equation (25) yields

$$\frac{1}{Z_L} = \frac{q_L}{p_R} = \left(\frac{1}{R_G} + \frac{1}{R_L} + C_L S\right) \tag{29}$$

Inserting this impedance in the block diagram of figure 2 and closing the inner loop gives the forward function

$$\frac{1}{\frac{1}{R_V} + \frac{1}{Z_L}} = \frac{R_S}{\tau_L S + 1} \tag{30}$$

$$\tau_L = R_S C_L \tag{31}$$

$$R_S = \frac{1}{\frac{1}{R_G} + \frac{1}{R_V} + \frac{1}{R_L}} \tag{32}$$

Combining the term (30) with the preceding term in figure 2 gives the following open loop transfer function

$$\frac{p_R}{\frac{p_L}{(1 - \alpha)} - p_R} = \frac{G_L(\tau_V S + 1)}{(\tau_L S + 1)\left(\frac{S^2}{\omega_P^2} + \frac{2\delta_P}{\omega_P} S + 1\right)} \tag{33}$$

where

$$G_L = \frac{R_S A_P K_V(1 - \alpha)}{K_{SP}(1 + \beta)} \tag{34}$$

In the case of closely coupled pump, regulator and load orifice the capacitance due to fluid compressibility may be so small that $1/\tau_L >> \omega_P$ in which case equation (33) reduces to

$$\frac{P_R}{\frac{P_L}{(1-\alpha)} - P_R} = \frac{G_L(\tau_V S + 1)}{\left(\frac{S^2}{\omega_P^2} + \frac{2f_P}{\omega_P} S + 1\right)} \tag{35}$$

The closed loop transfer function obtained from equation (35) is

$$\frac{P_R}{P_L}(1-\alpha) = \frac{\frac{G_L}{G_L+1}(\tau_V S + 1)}{\left(\frac{S^2}{\omega_R^2} + \frac{2\delta_R}{\omega_R} S + 1\right)} \tag{36}$$

where

$$\omega_R = \sqrt{\frac{K_{SP}(1+\beta) + R_S K_V A_P (1-\alpha)}{M_P}} \tag{37}$$

$$\delta_R = \frac{K_{DP} + R_S A_P^2 (1-\alpha)}{2\sqrt{M_P[K_{SP}(1+\beta) + R_S K_V A_P (1-\alpha)]}} \tag{38}$$

Equation (38) illustrates that damping is generated in the closed loop and therefore damping in a pressure regulator does not go to zero as the mechanical damping goes to zero. Experimental verification of the existence of this damping property is given in (1). It is illustrated by equation (34) and (37) further, that under the condition of close regulation ($G_L >> 1$) the dynamic response (ω_R) is essentially independent of the total of mechanical and flow force spring rates. This observation is supported by the data in (1). The analysis given in (1) is based on the representation of the system of figure 1 by a passive electrical network. This model gave good agreement with experimental regulator response for the case of the resistive load but cannot represent the unstable state.

For zero mechanical damping, the open loop transfer function of the capacitive plus resistive load case, equation (33) reduces to

$$\frac{P_R}{\frac{P_L}{(1-\alpha)} - P_R} = \frac{G_L(\tau_V S + 1)}{(\tau_L S + 1)\left(\frac{S^2}{\omega_P^2} + 1\right)} \tag{39}$$

A derivation of equation (39) is given in (2) which comprehensively treats the sensing line restrictor method of stabilization, but does not examine the closed loop properties of this transfer function.

Summing the numerator and the denominator of equation (39) gives the characteristic equation of the closed loop

$$\frac{\tau_L}{\omega_P^2} S^3 + \frac{1}{\omega_P^2} S^2 + (\tau_L + G_L\tau_V)S + G_L + 1 = 0 \tag{40}$$

Applying Routh's stability criterion to this equation, the stability limit given is

$$(G_L + 1)\tau_L < \tau_L + G_L\tau_V \tag{41}$$

From equations (12), (31), and (34)

$$\tau_L + G_L\tau_V = R_S\left[C_L + \frac{A_P^2(1-\alpha)}{K_{SP}(1+\beta)}\right] \tag{42}$$

It can be seen from equation (42) that for the case of a load having a large capacity and a regulator having a small piston area and large spring rate the condition $\tau_L >> G_L\tau_V$ can occur, in which case criterion (41) reduces to $G_L < 0$, indicating that the system is unstable at any gain. However, the condition $\tau_L >> G_L\tau_V$ is not likely to occur in a hydraulic system and, in fact, the required magnitude of C_L may not be physically realizable through compressibility because of distributed parameter effects in large fluid volumes. In hydraulic system, the condition $G_L\tau_V >> \tau_L$ is very likely to occur along with the complementary condition $G_L >> 1$, in which case criterion (41) reduces to

$$\tau_V > \tau_L \tag{43}$$

In terms of the open loop transfer function (39), this limit states that the lead time constant must be greater than the lag time constant for system stability.

Substituting equations (12) and (31) in (43) gives

$$K_V < \frac{A_P}{R_S C_L} \tag{44}$$

Under usual operating conditions the regulated pressure is much lower than the pump dead-head pressure and the following condition exists

$$\frac{1}{R_G} << \frac{1}{R_V} + \frac{1}{R_L} \tag{45}$$

Under this condition and with the load resistor being an orifice

$$R_S = \frac{1}{\frac{1}{R_V} + \frac{1}{R_L}} = \frac{2P_R}{Q_V + Q_L} = \frac{2P_R}{Q_G} \tag{46}$$

Substituting equations (4) and (46) in limit (44), yields the valve gain limit

$$W < \frac{A_P Q_G}{2DP_R^{3/2} C_L} \tag{47}$$

For C_L derived from oil compressibility

$$C_L = \frac{V}{B} \tag{48}$$

and the valve gain limit is

$$W < \frac{A_P Q_G B}{2DVP_R^{3/2}} \tag{49}$$

As a design equation the valve gain limit can be written

$$W = \frac{A_P Q_G B}{2\theta DVP_R^{3/2}} \tag{50}$$

where

$\theta > 1$ (gain ratio margin)

A Routh's criterion analysis of the characteristic equation of the pressure regulator with a purely capacitive load is made in (3). The purely capacitive load is the present case with $R_L = \infty$. In (3), terms that are given in the forming equation are inexplicably

omitted from the characteristic equation; therefore, equation (50) is not derived and the erroneous conclusion is drawn that frictional damping is always required.

Equation (50) indicates that with a fixed pump output, the regulator with a fixed value of W will be stable at all load flows. If the regulator is used with a variable output pump, stability can be maintained at all pump outputs by using a gain set by equation (50) with Q_G at the lowest expected value. This procedure may not be practical when the Q_G range is large. For a large Q_G range a variable valve gain will be required. The logarithmic valve port, which is derived below can be used for this purpose.

At zero load flow, the valve flow is expressible by the orifice equation

$$Q_G = DA_V\sqrt{P_R} \tag{51}$$

Substituting equation (51) in equation (50) and making the substitution

$$W = \frac{dA_V}{dX_P}$$

equation (50) becomes

$$\frac{dA_V}{dX_P} = \left(\frac{A_P B}{2\theta V P_R}\right) A_V \tag{52}$$

or

$$\frac{dA_V}{A_V} = \left(\frac{A_P B}{2\theta V P_R}\right) dX_P \tag{53}$$

Integrating both sides

$$\log_e A_V = \left(\frac{A_P B}{2\theta V P_R}\right) x_P + K \tag{54}$$

By substituting equation (51) in equation (52) it is seen that the valve gain is varied with Q_G in accordance with equation (50). For load flows greater than zero, the valve flow and A_V are reduced, which produces a reduction in valve gain according to equation (52). The gain margin therefore increases with load flow. The effect of loop gain reduction on system dynamic response and droop at the highest expected value of load flow should be taken into account in the use of the logarithmic valve port.

Relief Valve Pressure Regulator with a Parallel Capacitive Plus Resistive Load and a Tuned Stabilizer

The flow equilibrium in the impedance junction shown in figure 4, assuming condition (45) is

$$q_L + q_C + q_R + q_D = 0 \tag{55}$$

where

$$q_C = -C_L S p_R \tag{56}$$

$$q_R = -\frac{1}{R_L} p_R \tag{57}$$

$$q_D = -A_D S x_D \tag{58}$$

The stabilizer force equilibrium is

$$(M_D S^2 + K_{DD} S + K_{SD}) x_D - A_D p_R = 0 \tag{59}$$

or

$$x_D = \frac{A_D/K_{SD}}{\left(\frac{S^2}{\omega_D^2} + \frac{2\delta_D}{\omega_D} S + 1\right)} p_R \tag{60}$$

where

$$\omega_D = \sqrt{\frac{K_{SD}}{M_D}} \tag{61}$$

$$\delta_D = \frac{K_{DD}}{2\sqrt{K_{SD} M_D}} \tag{62}$$

From equations (58) and (60)

$$q_D = -\frac{C_{DS}}{\left(\frac{S^2}{\omega_D^2} + \frac{2\delta_D}{\omega_D} S + 1\right)} p_R \tag{63}$$

where

$$C_D = \frac{A_D^2}{K_{SD}} \tag{64}$$

Substituting equations (56), (57), and (63) in equation (55) yields

$$\frac{q_L}{p_R} = \frac{1}{z_L} =$$

$$\left\{\frac{R_L C_L}{\omega_D^2} S^3 + \left(\frac{1}{\omega_D^2} + \frac{2\delta_D}{\omega_D} R_L C_L\right) S^2 + \left[R_L (C_L + C_D) + \frac{2\delta_D}{\omega_D}\right] S + 1\right\} \Bigg/ \left[R_L \left(\frac{S^2}{\omega_D^2} + \frac{2\delta_D}{\omega_D} S + 1\right)\right] \tag{65}$$

Inserting this impedance in the block diagram of figure 2 and closing the inner loop gives the forward function

$$\frac{R_V z_L}{R_V + z_L} =$$

$$\left[R_S \left(\frac{S^2}{\omega_D^2} + \frac{2\delta_D}{\omega_D} S + 1\right)\right] \Bigg/ \left\{\frac{\tau_L}{\omega_D^2} S^3 + \left(\frac{1}{\omega_D^2} + \frac{2\delta_D}{\omega_D} \tau_L\right) S^2 + \left(\tau_D + \tau_L + \frac{2\delta_D}{\omega_D}\right) S + 1\right\} \tag{66}$$

where

$$\tau_D = R_S C_D \tag{67}$$

Combining the term (66) with the preceding term in figure 2 gives the following open loop transfer function

$$\frac{p_R}{\frac{p_L}{(1-\alpha)} - p_R} =$$

$$\left[G_L (\tau_V S + 1) \left(\frac{S^2}{\omega_D^2} + \frac{2\delta_D}{\omega_D} S + 1\right)\right] \Bigg/ \left\{\left(\frac{S^2}{\omega_P^2} + \frac{2\delta_P}{\omega_P} S + 1\right) \times \left[\frac{\tau_L}{\omega_D^2} S^3 + \left(\frac{1}{\omega_D^2} + \frac{2\delta_D}{\omega_D} \tau_L\right) S^2 + \left(\tau_D + \tau_L + \frac{2\delta_D}{\omega_D}\right) S + 1\right]\right\} \tag{68}$$

If the stabilizer factor in the numerator is made to cancel the spring-mass valve factor in the denominator the open loop transfer function reduces to

$$\frac{P_R}{\frac{P_R}{(1-\alpha)} - P_L} = [G_L(\tau_V S + 1)] \Bigg/ \left\{ \left[\frac{\tau_L}{\omega_D^2} S^3 + \left(\frac{1}{\omega_D^2} + \frac{2\delta_D}{\omega_D} \tau_L \right) S^2 + \left(\tau_D + \tau_L + \frac{2\delta_D}{\omega_D} \right) S + 1 \right] \right\} \quad (69)$$

Summing the numerator and denominator of transfer function (69) gives the following system characteristic equation

$$\frac{\tau_L}{\omega_D^2} S^3 + \left(\frac{1}{\omega_D^2} + \frac{2\delta_D}{\omega_D} \tau_L \right) S^2 + \left(\tau_D + \tau_L + \frac{2\delta_D}{\omega_D} + G_L \tau_V \right) S + G_L + 1 = 0 \quad (70)$$

Applying Routh's stability criterion to this equation, gives the stability limit

$$(G_L + 1) \frac{\tau_L}{\omega_D^2} < \left(\frac{1}{\omega_D^2} + \frac{2\delta_D}{\omega_D} \tau_L \right) \left(\tau_D + \tau_L + \frac{2\delta_D}{\omega_D} + G_L \tau_V \right) \quad (71)$$

Rearranging terms gives

$$G_L < \frac{\frac{\tau_D}{\tau_L} + 2\delta_D \left[\frac{1}{\omega_D \tau_L} + \omega_D (\tau_D + \tau_L + \tau_P) + 2\delta_D \right]}{1 - \frac{\tau_V}{\tau_L}} \quad (72)$$

In the condition establishing this relationship $\delta_D = \delta_P$ is implied, it is therefore meaningless to consider large values of δ_D; however, it is consistent and practical to set $\delta_D = 0$. In this case criterion (72) reduces to

$$G_L < \frac{\tau_D}{\tau_L - \tau_V} \quad (73)$$

From equations (12) and (34)

$$G_L \tau_V = \frac{R_S A_P^2 (1-\alpha)}{K_{SP}(1+\beta)} = \tau_P \quad (74)$$

Substituting equations (12), (31), (67), and (74) in criterion (73) yields

$$K_V < \frac{A_P}{R_S C_L} \left[1 + \frac{K_{SP} A_D^2 (1+\beta)}{K_{SD} A_P^2 (1-\alpha)} \right] \quad (75)$$

Substituting equations (4), (46), and (48) yields

$$W < \frac{A_P Q_G B}{2DVP_R^{3/2}} \left[1 + \frac{K_{SP} A_D^2 (1+\beta)}{K_{SD} A_P^2 (1-\alpha)} \right] \quad (76)$$

Comparison of criteria (76) and (49) indicates that a pressure regulator that is unstable with a capacitive load can be made stable by the tuned stabilizer or that the allowable valve gain is increased by a factor $\{1 + [K_{SP} A_D^2 (1+\beta)]/[K_{SD} A_P^2 (1-\alpha)]\}$.

Criterion (76) is based on exact cancelation of the spring-mass valve factor by the stabilizer factor. Exact tuning is usually not practical. It is therefore important to examine the effect of the ratio ω_D/ω_P. For $(\omega_D/\omega_P) \gg 1$ or $(\omega_D/\omega_P) \ll 1$ the stabilizer is either effectively out of the circuit or is combined with the load capacity. Because of the many variables involved, a general derivation of the limits of ω_D/ω_P has not been attempted. Instead, a Bode diagram analysis of transfer function (68) has been made. This analysis, which utilized conditions thought to be in common practice, indicates that the gain margin given by criterion (76) is substantially provided when ω_D/ω_P is placed within the limits $0.5 < \omega_D/\omega_P < 1.5$.

The Bode diagram plot of transfer function (68) can be facilitated by the approximate factorization of the cubic term. The factorization is based on the following conditions

$$\frac{1}{\tau_L} \gg 2\delta_D \omega_D$$

$$\tau_D \gg \tau_L$$

$$\frac{\omega_D^2 \tau_D}{\tau_L} \gg \frac{1}{\tau_D \tau_L}$$

Under these conditions the factors of the cubic in transfer function (68) are

$$(\tau_D S + 1) \left(\frac{S^2}{\omega_A^2} + \frac{2\delta_A}{\omega_A} S + 1 \right)$$

where

$$\omega_A = \omega_D \sqrt{\frac{\tau_D}{\tau_L}} \quad (77)$$

$$\delta_A = \frac{1}{2\omega_D \sqrt{\tau_D \tau_L}} \quad (78)$$

and transfer function (68) becomes

$$\frac{P_R}{\left(\frac{P_L}{1-\alpha} - P_R \right)} = \left[G_L(\tau_V S + 1) \left(\frac{S^2}{\omega_D^2} + \frac{2\delta_D}{\omega_D} S + 1 \right) \right] \Bigg/ \left[(\tau_D S + 1) \times \left(\frac{S^2}{\omega_A^2} + \frac{2\delta_A}{\omega_A} S + 1 \right) \left(\frac{S^2}{\omega_P^2} + \frac{2\delta_P}{\omega_P} S + 1 \right) \right] \quad (79)$$

It is a convenience in the Bode diagram to normalize transfer function (79) in terms of ω/ω_P. Transfer function (79) so normalized and converted to the frequency domain is

$$\frac{P_R}{\left[\frac{P_L}{(1-\alpha)} - P_R\right]} =$$

$$\left\{G_L\left[1 + J(\tau_V\omega_P)\frac{\omega}{\omega_P}\right]\left[1 - \left(\frac{\omega_P}{\omega_D}\right)^2\left(\frac{\omega}{\omega_P}\right)^2 + J\left(2\delta_D\frac{\omega_P}{\omega_D}\right)\frac{\omega}{\omega_P}\right]\right\} \Bigg/ \left\{\left[1 + J(\tau_D\omega_P)\frac{\omega}{\omega_P}\right]\right.$$

$$\times\left[1 - \left(\frac{\omega_P}{\omega_A}\right)^2\left(\frac{\omega}{\omega_P}\right)^2 + J\left(\frac{2\delta_A\omega_P}{\omega_A}\right)\frac{\omega}{\omega_P}\right]\left[1 - \left(\frac{\omega}{\omega_P}\right)^2\right.$$

$$\left.\left. + J2\delta_P\frac{\omega}{\omega_P}\right]\right\} \tag{80}$$

Relief Valve Pressure Regulator with a Parallel Capacitive Plus Inductive Load

In some load moving hydraulic systems the hydraulic load is equivalent to the circuit shown in figure 4 where the stabilizer spring is omitted and $R_L = \infty$.

In the absence of a spring restraint and neglecting damping, equation (63) reduces to

$$q_D = -\frac{1}{L_D S} \tag{81}$$

where

$$L_D = \frac{M_D}{A_D^2} \tag{82}$$

Substituting equations (56) and (81) in equation (55) yields

$$\frac{1}{Z_L} = \frac{L_D C_L S^2 + 1}{L_D S} \tag{83}$$

and

$$\frac{R_V Z_L}{R_V + Z_L} = R_V\left(\frac{\frac{2\delta_L}{\omega_L}S}{\frac{S^2}{\omega_L^2} + \frac{2\delta_L}{\omega_L}S + 1}\right) \tag{84}$$

where

$$\omega_L = \frac{1}{\sqrt{L_D C_L}} \tag{85}$$

$$\delta_L = \frac{1}{2R_V}\sqrt{\frac{L_D}{C_L}} \tag{86}$$

Combining the term (84) with the preceding term in figure 2 gives the following open loop transfer function

$$\frac{P_R}{\frac{P_L}{(1-\alpha)} - P_R} = \frac{G_L\tau_{DL}S(\tau_V S + 1)}{\left(\frac{S^2}{\omega_P^2} + \frac{2\delta_P}{\omega_P}S + 1\right)\left(\frac{S^2}{\omega_L^2} + \frac{2\delta_L}{\omega_L}S + 1\right)} \tag{87}$$

where

$$\tau_{DL} = \frac{L_D}{R_V} \tag{88}$$

Neglecting valve damping the system characteristic equation is from transfer function (87)

$$S^4 + 2\delta_L\omega_L S^3 + (\omega_L^2 + \omega_P^2 + \omega_L^2\omega_P^2 G_L\tau_V\tau_D)S^2$$

$$+ (2\delta_L\omega_L\omega_P^2 + G_L\tau_D\omega_L^2\omega_P^2)S + \omega_L^2\omega_P^2 = 0 \tag{89}$$

Routh's criterion applied to equation (89) and reduced through consideration of the relative magnitude of terms gives the following stability limit

$$W < \frac{A_P Q_G B}{2DVP_R^{3/2}}\left[\frac{M_P A_D^2}{M_D A_P^2} + 1 + \frac{VK_{SP}(1+\beta)}{BA_P^2(1-\alpha)}\right] \tag{90}$$

A dynamic analysis of a poppet valve type relief valve pressure regulator with a parallel capacitive plus inductive load and a Routh's stability analysis of the derived characteristic equation are given in (4) and reproduced in (5). The mechanism by which the sensing piston, which is integral with the valve element, pumps flow at a rate proportional to the velocity of the valve element is obscure in the case of the poppet valve and was neglected. For this reason the important damping term that is produced by this pumped flow is not included in the equations given in (4) and no definitive stability criterion, such as (90) is derived.

Criterion (90) presents interesting stabilizing characteristics but a springless piston would be statically unstable and therefore could not be used as a stabilizer. For this reason further consideration of it is outside of the scope of this paper.

Relief Valve Pressure Regulator in a Counterbalance Circuit

In the counterbalance valve circuit shown in figure 5, the pump of the previous circuits is replaced by a loaded piston and a control orifice. The flow generator impedance is more complex than resistive as considered previously and the load impedance is purely capacitive.

The flow equilibrium in the impedance junction of the flow generator is

$$q_M + q_G + q_C = 0 \tag{91}$$

where

$$q_M = A_M S x_M \tag{92}$$

$$q_G = -\frac{P_M}{R_G} + \frac{P_R}{R_G}$$

$$q_C = -\frac{V_M}{B}Sp_M \tag{94}$$

Assuming a constant actuator load, the piston force equilibrium is

$$(M_M S^2 + K_{DM}S)x_M + A_M p_M = 0 \tag{95}$$

or

$$x_M = -\frac{A_M/K_{DM}}{S\left(\frac{M_M}{K_{DM}}S + 1\right)}p_M \tag{96}$$

From equations (92) and (96)

$$q_M = -\frac{A_M^2/K_{DM}}{\left(\frac{M_M}{K_{DM}} S + 1\right)} P_M \tag{97}$$

Substituting equations (93), (94), and (97) in equation (91) yields

$$\frac{P_M}{P_R} = \frac{M_M S + K_{DM}}{\frac{M_M R_G V_M}{B} S^2 + \left(\frac{R_G V_M K_{DM}}{B} + M_M\right) S + (R_G A_M^2 + K_{DM})} \tag{98}$$

Neglecting the K_{DM} terms, transfer function (98) reduces to

$$\frac{P_M}{P_R} = \frac{\tau_M S}{\frac{S^2}{\omega_M^2} + \frac{2\delta_M}{\omega_M} S + 1} \tag{99}$$

where

$$\tau_M = \frac{M_M}{A_M^2 R_G} \tag{100}$$

$$\omega_M = \sqrt{\frac{A_M^2 B}{M_M V_M}} \tag{101}$$

$$\delta_M = \frac{1}{2R_G}\sqrt{\frac{M_M B}{A_M^2 V_M}} \tag{102}$$

The flow generator impedance is

$$Z_G = \frac{P_R}{q_G} = \frac{P_R R_G}{P_R - P_M} = \frac{R_G}{1 - \frac{P_M}{P_R}} \tag{103}$$

Substituting equation (99) in equation (103) yields

$$\frac{1}{Z_G} = \frac{1}{R_G}\left[\frac{\frac{S^2}{\omega_M^2} + 1}{\frac{S^2}{\omega_M^2} + \frac{2\delta_M}{\omega_M} S + 1}\right] \tag{104}$$

For a purely capacitive load, the load impedance is

$$Z_L = \frac{1}{C_L S} \tag{105}$$

The parallel sum of the flow generator and load impedance is

$$\frac{Z_G Z_L}{Z_G + Z_L} = \frac{1}{\frac{1}{Z_G} + \frac{1}{Z_L}} =$$

$$\left[R_G\left(\frac{S^2}{\omega_M^2} + \frac{2\delta_M}{\omega_M} S + 1\right)\right] \Bigg/ \left\{\left[\frac{R_G C_L}{\omega_M^2} S^3 + \left(\frac{2\delta_M R_G C_L}{\omega_M} + \frac{1}{\omega_M^2}\right) S^2 + R_G C_L S + 1\right]\right\} \tag{106}$$

Inserting this impedance in the block diagram of figure 2 and closing the inner loop gives the forward function

$$\frac{1}{\frac{1}{R_V} + \frac{1}{Z_L} + \frac{1}{Z_G}} =$$

$$\left[R_S\left(\frac{S^2}{\omega_M^2} + \frac{2\delta_M}{\omega_M} S + 1\right)\right] \Bigg/ \left\{\left[\frac{\tau_L}{\omega_M^2} S^3 + \left(\frac{1}{\omega_M^2} + \frac{2\delta_M}{\omega_M}\tau_L\right) S^2 + \left[\frac{2R_G\delta_M}{(R_V + R_G)\omega_M} + \tau_L\right] S + 1\right\}\right) \tag{107}$$

where

$$R_S = \frac{R_V R_G}{R_V + R_G} \tag{108}$$

Combining the term (107) with the preceding term in figure 2 gives the following open loop transfer function

$$\frac{P_R}{\frac{P_L}{(1 - \alpha)} - P_L} =$$

$$\left[G_L(\tau_V S + 1)\left(\frac{S^2}{\omega_M^2} + \frac{2\delta_M}{\omega_M} S + 1\right)\right] \Bigg/ \left(\left(\frac{S^2}{\omega_P^2} + \frac{2\delta_P}{\omega_P} S + 1\right) \times \left\{\frac{\tau_L}{\omega_M^2} S^3 + \left(\frac{1}{\omega_M^2} + \frac{2\delta_M}{\omega_M}\tau_L\right) S^2 + \left[\frac{2R_G\delta_M}{(R_V + R_G)\omega_M} + \tau_L\right] S + 1\right\}\right) \tag{109}$$

In the case of a closely coupled control orifice and counterbalance valve the τ_L terms in transfer function (109) can be neglected and the function reduces to

$$\frac{P_R}{\frac{P_R}{(1 - \alpha)} - P_R} =$$

$$\frac{G_L(\tau_V S + 1)\left(\frac{S^2}{\omega_M^2} + \frac{2\delta_M}{\omega_M} S + 1\right)}{\left(\frac{S^2}{\omega_P^2} + \frac{2\delta_P}{\omega_P} S + 1\right)\left[\frac{S^2}{\omega_M^2} + \frac{2R_G\delta_M}{(R_V + R_G)\omega_M} S + 1\right]} \tag{110}$$

In view of physical considerations in counterbalance valve use, it can be considered to be most probable that $\omega_P >> \omega_M$, in which case the two motor quadratic factors effectively cancel and the open loop transfer function (110) reduces to (35) and equations (37) and (38) can be used in initial design or selection.

When close coupling is not possible the τ_L terms cannot be neglected. In this case the cubic

factor can be factored by numerical methods and the stability margin determined by a Bode diagram. If a stability problem is indicated, it is likely that τ_L is large enough so that

$$\left[\frac{2R_G\delta_M}{(R_V + R_G)\omega_M} + \tau_L\right] \approx \left(\frac{2\delta_M}{\omega_M} + \tau_L\right)$$

In this case, the approximate factors of the cubic factor in function (109) are

$$(\tau_L S + 1)\left(\frac{S^2}{\omega_M^2} + \frac{2\delta_M}{\omega_M} S + 1\right)$$

Substituting these factors for the cubic factor, open loop transfer function (109) becomes

$$\frac{p_R}{\frac{p_L}{1-\alpha} - p_R} = \frac{G_L(\tau_V S + 1)}{(\tau_L S + 1)\left(\frac{S^2}{\omega_P^2} + \frac{2\delta_P}{\omega_P} S + 1\right)} \quad (111)$$

Equation (111) is identical to equation (32). It can therefore be expected that the logarithmic valve port and the tuned stabilizer can be used effectively in counterbalance valve circuits.

Reducing Valve Regulator Dynamics

Basic Circuit and Valve Configuration

A fundamental configuration of a pressure regulator of the reducing valve type coupled to a pressure generator energized system is illustrated in figure 6. The piston and sleeve assembly is configured for the pressure reducing function but otherwise is the same as that shown in figure 1. The pressure generator and circuit load are treated as general impedances.

Pressure and Flow Equations

The flow equilibrium in the regulated pressure function can be written

$$q_V + q_P + q_L = 0 \quad (112)$$

where

$$q_V = K_V x_P - \frac{1}{R_V} p_R + \frac{1}{R_V} p_S \quad (113)$$

$$q_P = A_P S x_P \quad (114)$$

$$q_L = -\frac{1}{Z_L} p_R \quad (115)$$

If the impedance of the pressure generator is greater than zero, then

$$p_S = -Z_S q_V \quad (116)$$

Substituting equation (116) in equation (113) gives

$$q_V = \frac{K_V R_V}{(R_V + Z_S)} x_P - \frac{p_R}{(R_V + Z_S)} \quad (117)$$

Substituting equations (114), (115), and (117) in equation (112) yields

$$p_R = \frac{K_V\left[\tau_V\left(1 + \frac{Z_S}{R_V}\right)S + 1\right]}{\left[\frac{1}{R_V} + \frac{1}{Z_L}\left(1 + \frac{Z_S}{R_V}\right)\right]} x_P \quad (118)$$

Force Equations

In terms of the force equilibrium given in equation (13), and taking the direction of force in the valve opening direction as positive, the forces are

$$f_P = -A_P(p_R - p_L) \quad (119)$$

$$f_S = -K_{SP} x_P \quad (120)$$

$$f_I = -M_P S^2 x_P \quad (121)$$

$$f_D = -K_{DP} S x_P \quad (122)$$

$$f_q = -\frac{C_1 K_V (R_V - Z_S)}{(R_V + Z_S)} x_P + \frac{2C_1}{(R_V + Z_S)} p_R \text{ (derived in Appendix B)} \quad (123)$$

Substituting equations (118)-(123) in equation (13) yields

$$x_P = \frac{\frac{A_P\left(1 - \frac{R_V\alpha}{R_V + Z_S}\right)}{\frac{K_{SP}\left[1 + \left(\frac{R_V - Z_S}{R_V + Z_S}\right)\beta\right]}{}}\left[p_R - \frac{p_L}{\left(1 - \frac{R_V\alpha}{R_V + Z_S}\right)}\right]}{\left(\frac{S^2}{\omega_P^2} + \frac{2\delta_P}{\omega_P} S + 1\right)} \quad (124)$$

where

$$\omega_P = \sqrt{\frac{K_{SP}\left[1 + \frac{(R_V - Z_S)\beta}{(R_V + Z_S)}\right]}{M_P}} \quad (125)$$

$$\delta_P = \frac{K_{DP}}{2\sqrt{K_{SP} M_P\left[1 + \frac{(R_V - Z_S)\beta}{R_V + Z_S}\right]}} \quad (126)$$

Equations (118) and (123) combined in block diagram form is shown in figure 7.

Because Z_S can contain dynamic terms the analysis of the reducing valve could be considerably more complex than the relief valve. However, in most applications $Z_S << R_V$, in which case the block diagram reduces to that of figure 2. Therefore, in most cases, the stabilization methods of the relief type pressure regulator apply to the reducing valve type.

Reducing Valve Pressure Regulator With a Parallel Capacitive Plus Resistive Load

The stability criterion for this case is given by equation (44) where in this case

$$K_V = DW\sqrt{P_S - P_R} \quad (127)$$

$$R_V = \frac{2(P_S - P_R)}{Q_L} \quad (128)$$

$$R_L = \frac{2P_R}{Q_L} \quad (129)$$

and

$$\frac{1}{R_S} = \frac{1}{R_V} + \frac{1}{R_L} = \frac{Q_L P_S}{2P_R(P_S - P_R)} \quad (130)$$

Substituting equations (127) and (130) in equation (44) gives the general stability criterion

$$W < \frac{A_P Q_L P_S}{2DC_L P_R (P_S - P_R)^{3/2}} \quad (131)$$

or as a design equation

$$W = \frac{A_P Q_L P_S}{2D\theta C_L P_R (P_S - P_R)^{3/2}} \qquad (132)$$

and for C_L derived from oil compressibility

$$W = \frac{A_P Q_L P_S B}{2D\theta V P_R (P_S - P_R)^{3/2}} \qquad (133)$$

The term $P_S/[P_R(P_S - P_R)]$ has its minimum value at $P_R = (2/5)\ P_S$.

In an analysis of stability of the reducing valve under sensing line restrictor stabilization, (6) draws the conclusion "the most critical operating point for stability is at zero load flow and $(P_S - P_R) = (1/2)\ P_S$." In view of Q_L in the numerator and of the minimum value of the pressure term, criterion (131) is in close agreement with this conclusion.

Inserting the derived value $P_R = (2/5)\ P_S$ in equation (133) gives a design equation in terms of P_S alone

$$W = \frac{2.69 A_P B Q_L}{\theta D V P_S^{3/2}} \qquad (134)$$

A valve that is designed in accordance with equation (134) will have a gain ratio margin $\geq \theta$ at the design value of Q_L at any setting of P_R, but the margin will reduce proportionally as Q_L is lowered below the design value.

In the reducing valve circuit $Q_V = Q_L$ and therefore the relationsnip between load flow and regulator valve area is

$$Q_L = DA_V\sqrt{P_S - P_R} \qquad (135)$$

Substituting equation (135) in equation (133) and substituting $W = (dA_V)/dX_P$ gives

$$\frac{dA_V}{dX_P} = \left[\frac{A_P B P_S}{2\theta V P_R (P_S - P_R)}\right] A_V \qquad (136)$$

The term $P_S/[P_R(P_S - P_R)]$ has its minimum value at $P_R = (1/2)\ P_S$. Inserting this value in equation (136) gives

$$\frac{dA_V}{dX_P} = \left(\frac{2A_P B}{\theta V P_S}\right) A_V \qquad (137)$$

or

$$\frac{dA_V}{A_V} = \left(\frac{2A_P B}{\theta V P_S}\right) dX_P \qquad (138)$$

Integrating both sides

$$\log_e A_V = \left(\frac{2A_P B}{\theta V P_S}\right) x_P + K \qquad (139)$$

A valve designed by equation (139) will have a fixed gain ratio margin over a range of Q_L. Limitation of space and of fabrication limit the range ratio to approximately 10.

Reducing Valve Pressure Regulator with a Parallel Capacitive Plus Resistive Load and a Tuned Stabilizer

The stability criterion for this case under the condition of cancelation of the spring-mass valve factor by the stabilizer factor is given in criterion (75). Substituting equations (127) and (130) in criterion (75) yields

$$W < \frac{A_P Q_L B P_S}{2DVP_R (P_S - P_R)^{3/2}} \left[1 + \frac{K_{SP} A_D^2 (1 + \beta)}{K_{SD} A_P^2 (1 - \alpha)}\right] \qquad (140)$$

Setting $P_R = (2/5)\ P_S$ gives the design equation

$$W = \frac{2.69 A_P B Q_L}{\theta D V P_S^{3/2}} \left[1 + \frac{K_{SP} A_D^2 (1 + \beta)}{K_{SD} A_P^2 (1 - \alpha)}\right] \qquad (141)$$

Response to Load Impedance Change

Basic Relationships

The principal impedance element that is subject to sudden or input generated change is the resistive element which commonly results from an orifice area change. The load flow change that results from an impedance change and from the accompanying change in regulated pressure may be expressed

$$q_L = \frac{P_R}{Z_L} + \frac{2Q_L}{2Z_L} z_L \qquad (143)$$

and in this case

$$z_L = \frac{2Z_L}{2R_L} \cdot \frac{2R_L}{2A_L} a_L \qquad (144)$$

The product $\{(\partial Q_L/\partial Z_L) \cdot (\partial Z_L/\partial R_L) \cdot (\partial R_L/\partial A_L)\} = (\partial Q_L/\partial A_L = D\sqrt{P_R} = K_A$.

Equation (143) can then be written

$$q_L = \frac{P_R}{Z_L} + K_A a_L \qquad (145)$$

The generalized block diagram of figure 2 modified to incorporate the perturbation (a_L) is shown in figure 8. Figure 9 shows the reduction of the figure 8 diagram obtained by moving the term $(K_A a_L)$ to the feedback summing point. As in the determination of the stability margin from figure 2, the equation of load orifice area response are obtainable from figure 9 by substitution of the load impedance.

Pressure Regulator with a Parallel Capacitive Plus Resistive Load

The open loop transfer function of the regulator with this load is given by equation (33). The closed loop transfer function obtained equation (33) and multiplied by the orifice area input function that is given in figure 9 is

$$\frac{P_R}{a_L} = \frac{-\frac{K_A R_S}{(G_L + 1)}\left(\frac{S^2}{\omega_P^2} + \frac{2\delta_P}{\omega_P} S + 1\right)}{(a_3 S^3 + a_2 S^2 + a_1 S + 1)} \qquad (146)$$

where

$$a_3 = \frac{\tau_L}{(G_L + 1)\omega_P^2}$$

$$a_2 = \frac{1}{(G_L + 1)}\left(\frac{1}{\omega_P^2} + \frac{2\delta_P}{\omega_P}\tau_L\right)$$

$$a_1 = \frac{1}{(G_L + 1)}\left(\frac{2\delta_P}{\omega_P} + \tau_L + G_L\tau_V\right)$$

The load impedance for this case, incorporating R_G in R_L, is from equation (29)

$$z_L = \frac{R_L}{(R_L C_L S + 1)} \tag{147}$$

Substituting equation (147) in equation (145) gives

$$q_L = \left(\frac{R_L C_L S + 1}{R_L}\right) p_R + K_A a_L \tag{148}$$

Substituting equation (146) in equation (148) yields

$$\frac{q_L}{a_L} = \frac{K_a[R_L(G_L + 1) - R_S]}{R_L(G_L + 1)}\left(\frac{b_2 S^2 + b_1 S + 1}{a_3 S^3 + a_2 S^2 + a_1 S + 1}\right) \tag{149}$$

where

$$b_2 = \left\{\frac{(R_L - R_S)}{[R_L(G_L + 1) - R_S]\omega_P^2}\right\}$$

$$b_1 = \left\{\frac{1}{[R_L(G_L + 1) - R_S]}\right\}\left[\frac{2\delta_P}{\omega_P}(R_L - R_S) + R_L G_L \tau_V\right]$$

While load flow (q_L) is not a physical input in this system, the variation of regulated pressure (p_R) with load flow (q_L) in steady state is a measure of performance. In steady state, equations (146) and (149) reduce to respectively,

$$\frac{p_R}{a_L} = -\frac{K_A R_S}{(G_L + 1)} \tag{150}$$

$$\frac{q_L}{a_L} = \frac{K_A[R_L(G_L + 1) - R_S]}{R_L(G_L + 1)} \tag{151}$$

From equations (150) and (151)

$$\frac{p_R}{q_L} = -\frac{R_S R_L}{[R_L(G_L + 1) - R_S]} \tag{152}$$

Substituting equation (34) in equation (152) yields

$$\frac{p_R}{q_L} = -\frac{1}{\dfrac{A_P K_V(1 - \alpha)}{K_{SP}(1 + \beta)} + \dfrac{1}{R_S} - \dfrac{1}{R_L}} \tag{153}$$

In essentially all cases

$$\frac{1}{R_S} - \frac{1}{R_L} << \frac{A_P K_V(1 - \alpha)}{K_{SP}(1 - \beta)}$$

in which case, the droop equation becomes

$$\frac{p_R}{q_L} = -\frac{K_{SP}(1 + \beta)}{A_P K_V(1 - \alpha)} \tag{154}$$

In view of the common block diagram, equations (146), (149), and (154) apply to both types of regulators. This concept is supported by the agreement of equation (154) with the reducing valve droop equation that is derived and experimentally verified in (6).

Pressure Regulator with a Parallel Capacitive Plus Resistive Load and a Tuned Stabilizer

The open loop transfer function of the regulator with this load is given by equation (68). The closed loop transfer function obtained from equation (68) and multiplied by the orifice area input function that is given in figure 9 is

$$\frac{p_R}{a_L} = \frac{-\dfrac{K_A R_S}{(G_L + 1)}\left[\left(\dfrac{S^2}{\omega_P^2} + \dfrac{2\delta_P}{\omega_P}S + 1\right)\left(\dfrac{S^2}{\omega_D^2} + \dfrac{2\delta_D}{\omega_D}S + 1\right)\right]}{(c_5 S^5 + c_4 S^4 + c_3 S^3 + c_2 S^2 + c_1 S + 1)} \tag{155}$$

where

$$c_5 = \frac{\tau_L}{(G_L + 1)\omega_P^2\omega_D^2}$$

$$c_4 = \frac{1}{(G_L + 1)}\left[\frac{1}{\omega_P^2}\left(\frac{1}{\omega_D^2} + \frac{2\delta_D}{\omega_D}\tau_L\right) + \frac{2\delta_P}{\omega_P}\frac{\tau_L}{\omega_D^2}\right]$$

$$c_3 = \frac{1}{(G_L + 1)}\left[\frac{1}{\omega_P^2}\left(\tau_D + \tau_L + \frac{2\delta_D}{\omega_D}\right) + \frac{2\delta_P}{\omega_P}\left(\frac{1}{\omega_D^2} + \frac{2\delta_D}{\omega_D}\tau_L\right) + \frac{\tau_L}{\omega_D^2}\right]$$

$$c_2 = \frac{1}{(G_L + 1)}\left[\frac{1}{\omega_P^2} + \frac{1}{\omega_D^2} + \frac{2\delta_P}{\omega_P}\left(\tau_D + \tau_L + \frac{2\delta_D}{\omega_D}\right) + \frac{2\delta_D}{\omega_D}\tau_L + G_L\left(\frac{2\delta_D}{\omega_D}\tau_V + \frac{1}{\omega_D^2}\right)\right]$$

$$c_1 = \frac{1}{(G_L + 1)}\left[\frac{2\delta_P}{\omega_P} + \tau_D + \tau_L + \frac{2\delta_D}{\omega_D} + G_L\left(\tau_V + \frac{2\delta_D}{\omega_D}\right)\right]$$

Substituting the load impedance for this case given by equation (65) in equation (145) gives

$$q_L = \left(\left\{\frac{R_L C_L}{\omega_D^2}S^3 + \left(\frac{1}{\omega_D^2} + \frac{2\delta_D}{\omega_D}R_L C_L\right)S^2 + \left[R_L(C_L + C_D) + \frac{2\delta_D}{\omega_D}\right]S + 1\right\}\Big/\left[R_L\left(\frac{S^2}{\omega_D^2} + \frac{2\delta_D}{\omega_D}S + 1\right)\right]\right)p_R + K_A a_L \tag{156}$$

Substituting equation (155) in equation (156) yields

$$\frac{q_L}{a_L} = \frac{K_A[R_L(G_L + 1) - R_S]}{R_L(G_L + 1)} \times \left(\frac{d_4 S^4 + d_3 S^3 + d_2 S^2 + d_1 S + 1}{c_5 S^5 + c_4 S^4 + c_3 S^3 + c_2 S^2 + c_1 S + 1}\right) \tag{157}$$

where

$$d_4 = \frac{(R_L - R_S)}{\omega_P^2 \omega_D^2 [R_L(G_L + 1) - R_S]}$$

$$d_3 = \frac{(R_L - R_S)\left(\frac{2\delta_D}{\omega_D} + \frac{2\delta_P}{\omega_P}\right)}{\omega_P \omega_D [R_L(G_L + 1) - R_S]}$$

$$d_2 = \frac{R_L}{[R_L(G_L + 1) - R_S]}\left[\frac{(R_L - R_S)}{R_L}\left(\frac{1}{\omega_P^2} + \frac{1}{\omega_D^2} + \frac{4\delta_P\delta_D}{\omega_P\omega_D}\right) + G_L\left(\frac{2\delta_D}{\omega_D}\tau_V + \frac{1}{\omega_D^2}\right)\right]$$

$$d_1 = \frac{(R_L - R_S)}{[R_L(G_L + 1) - R_S]}\left(\frac{2\delta_P}{\omega_P} + \frac{2\delta_D}{\omega_D}\right)$$

Experimental Analysis

Apparatus

The apparatus was designed to explore the two major concepts developed in the mathematical analysis: (1) the stability limit under a parallel capacitive plus resistive load; and, (2) the stabilizing effect of the tuned stabilizer. The hydraulic circuit comprised: (1) a positive displacement pump coupled to a variable speed drive; (2) a relief valve pressure regulator configured as shown in figure 1; (3) an air charged piston accumulator (tuned stabilizer); and, (4) a manually adjustable load valve (orifice).

The mechanical and hydraulic constants of the apparatus are given in Table I.

TABLE I. - EXPERIMENTAL CONSTANTS

Pump displacement	0.65 in^3/rev (10.65 cm^3/rev)
Pump leakage resistance (R_G)	136 lb sec/in^5 (5.72 N sec/cm^5)
Drive motor speed range	600 to 6000 rpm
Regulator piston area	0.442 in^2 (2.852 cm^2)
Regulator variable orifice area gain	0.3 & 0.6 in. (0.762 & 1.524 cm)
Regulator loading spring rate	200 lb/in. (350.52 N/cm)
Weight or regulator piston plus one third of spring weight	0.259 lb (1.1521 N)
Stabilizer piston area	3.142 in^2 (20.26 cm^2)
Stabilizer piston weight	0.366 lb (1.628 N)
Stabilizer charge volume	60 in^3 (983 cm^3)
Minimum load volume	4.57 in^3 (74.89 cm^3)
Hydraulic fluid - jet fuel, SpGr	0.8
Fluid bulk modulus	160 000 lb/in^2 (110 316 N/cm^2)
Orifice dimensional constant (D)	100 in^2 sec/$\sqrt{lb}$ (3.059 cm^2 sec/$\sqrt{N}$)
Flow force coefficient ($C_1/\sqrt{P_R}$)	0.0043 lb sec/in^3 (0.00116 N sec/cm^3)

The regulator piston had a 1.00 in. (2.54 cm) engagement and 0.0005 in. (0.0127 mm) clearance with the sleeve. The loading spring was coupled to the piston through a ball pivot. The stabilizer piston seal was a pair of Teflon capped O rings.

Stability Limit Correlation

The stabilizer was not in the circuit and the system load volume was the minimum. The regulator variable orifice area gain was 0.3 in. (0.76 cm). The pump speed was brought to 6000 rpm with the regulator spring at minimum load. The regulated pressure was raised at this speed through loading spring adjustment. The pump speed was then slowly reduced until instability (as evidenced by regulated pressure oscillation) was observed. The values observed at the onset of oscillation are plotted in figure 10. The Q_G min line given by criterion (49) shows close agreement with the experimental values.

The independence of the stability limit upon load flow as indicated by equation (46) and criterion (49) was confirmed by the absence of the occurence of instability as load flow was varied from zero to pump output flow rate under a stable $P_R - Q_G$ value. Figure 11 shows a droop characteristic obtained in this process. As inferred by the droop line, stability was maintained through the point of regulator orifice closure (loss of regulation).

The slope of the droop line in figure 11 is -0.88 lb sec/in^5 (0.037 N sec/cm^5). The slope calculated by means of equation (154), at the mean values of P_R is -1.00 lb sec/in^5 (0.042 N sec/cm^5). This difference between measured and calculated droop would be barely detectable on the scale used in figure 11.

Tuned Stabilizer Effect Correlation

The oscillographic traces reproduced in figure 12 show the transition from stable pressure regulation to unstable oscillation when a tuned stabilizer is disengaged from a parallel capacitive plus resistive load. The disengagement was performed through release of the stabilizer air. It can be seen that the oscillation begins at the initiation of air pressure decay. The effect on the system is therefore detuning through loss of the stabilizer spring.

The conditions in this case are: W = 0.6 in. (1.524 cm); initial stabilizer charge pressure 45 lb/in^2 abs (31 N/cm^2); regulated pressure 380 lb/in^2 abs (262 N/cm^2); pressure drop across regulator variable orifice 295 lb/in^2 (203 N/cm^2); Q_G = 54 in^3/sec (885 cm^3/sec); and, Q_L = 20 in^3/sec (328 cm^3/sec).

The equations used to calculate the values given below are identified by the circled number.

(4) K_V = 1031 in^2/sec (6652 cm^2/sec)

(21) β = 0.381

(23) ω_P = 642 rad/sec

K_{SD} = 528 lb/in. (925 N/cm) { isothermal spring rate at P_R = 380 lb/in^2 abs (262 N/cm^2 abs)

(61) ω_D = 746 rad/sec

The volume of the stabilizer air compressed from the charge pressure value to regulated pressure value is 7.1 in^3 (116 cm^3). The hydraulic fluid volume added by this stabilizer is then 52.9 in^3 (867 cm^3) and the system load volume in this experimental case is 52.9 + 4.57 = 57.5 in^3 (942 cm^3).

The calculated values for the unstable case are:

(32) $R_S = 10.83$ lb sec/in^5 (0.4557 N sec/cm^5)

(31) (48) $\tau_L = 0.00389$ sec

(12) $\tau_V = 4.29 \times 10^{-4}$ sec

(34) $G_L = 18$

$$(33)\quad \frac{P_R}{\frac{P_L}{1-\alpha} - P_R} = \frac{18\left(1 + J0.275\,\frac{\omega}{\omega_P}\right)}{\left(1 + J2.5\,\frac{\omega}{\omega_P}\right)\left\{\left[1 - \left(\frac{\omega}{\omega_T}\right)^2\right] + J2\,\delta_P\,\frac{\omega}{\omega_P}\right\}} \qquad (33a)$$

The oscillographic record in figure 12 shows that the frequency of oscillation in the unstable state is 754 rad/sec, which is 1.174 ω_P. For a system represented by transfer function (33a) to oscillate in the unstable state at $\omega/\omega_P = 1.174$, the value of δ_P would have to be that with which the open loop transfer function produces 180 degree phase lag at this frequency ratio. The required value of δ_P is found to be 0.216, which falls within the expected range for this class of fit and spring load. The Bode diagram given by transfer function (33a) for $\delta_P = 0.216$ is plotted in figure 13. This diagram shows that the gain is 19.7 db above the stability limit.

The calculated values for the stable state are:

(64) (67) $\tau_D = 0.2024$ sec

(77) $\omega_A = 536$ rad/sec

(78) $\delta_A = 0.0239$

$\delta_D = 0.05$ (estimated)

$$(80)\quad \frac{P_R}{\frac{P_L}{1-\alpha} - P_R} = \frac{18\left(1 + J0.275\,\frac{\omega}{\omega_P}\right)\left\{\left[1 - 0.741\left(\frac{\omega}{\omega_T}\right)^2\right] + J0.086\,\frac{\omega}{\omega_P}\right\}}{\left(1 + J130\,\frac{\omega}{\omega_P}\right)\left\{\left[1 - 0.014\left(\frac{\omega}{\omega_P}\right)^2\right] + J0.0057\,\frac{\omega}{\omega_P}\right\}\left\{\left[1 - \left(\frac{\omega}{\omega_P}\right)^2\right] + J0.432\,\frac{\omega}{\omega_P}\right\}} \qquad (80a)$$

The Bode diagram given by transfer function (80a) is plotted in figure 14. This diagram shows a gain margin of 13.8 dB and a phase margin of 90°. The large phase margin is far more significant as the stability margin because the 180° crossover occurs at a very high frequency 920 Hz).

Conclusions

1. Direct acting, hydraulic pressure regulator can be provided which are stable without a frictional damper or a sensing line restrictor through geometric design and load compensation.

2. Linear dynamic analysis can be effectively employed in regulator geometry and load compensator design.

3. The technique of lead network stabilization (tuned stabilizer) can be employed in hydraulic systems.

4. Valve configurations that permit independent design selection of sensing piston area and regulator variable orifice area gain provide an important design capability.

5. A stable relief valve pressure regulator can be stable at all load flows up to an including full pump flow.

6. An unstable relief valve pressure regulator can be stabilized through an increase in pump flow rate.

7. A relief valve pressure regulator can remain stable over a wide range of pump flow rates through the use of a logarithmic variable orifice.

8. The stability of a relief valve pressure regulator in a counterbalance circuit can be improved through reduction of the fluid volume between the control valve and the pressure regulator.

9. At a given supply pressure, the reducing valve pressure regulator will be stable at all regulated pressure settings if it is stable at a regulated pressure setting equal to 2/5 of the supply pressure.

10. A reducing valve pressure regulator can be stable over a wide range of flow rates through the use of a logarithmic variable orifice and stable at all regulated pressure setting provided it is stable at a pressure setting equal to 1/2 of the supply pressure.

11. A grossly unstable hydraulic pressure regulator can be stabilized by the lead network effect of a tuned, air charged, piston type accumulator. The length of the accumulator should be no longer than that required by the air charge so that the stabilizer adds minimum fluid volume to the system.

Appendix A

Symbols

A_D	stabilizer piston area
A_L	load orifice area
a_L	perturbation in A_L
A_M	motor piston area
A_P	regulator piston area
A_V	regulator variable orifice area
a_V	perturbation in A_V
B	bulk modulus of working fluid
C_1	flow force flow coefficient
C_2	flow force pressure coefficient
C_D	stabilizer capacitance
C_L	load capacitance
C_V	orifice velocity coefficient
D	orifice dimensional constant
F_Q	flow force
f_D	damping force

f_I inertia force

f_P pressure force

f_Q flow force

f_S spring force

G_L loop gain

g acceleration of gravity

e base of natural logarithms

J $\sqrt{-1}$

K_A load orifice area flow gain

K_{DD} stabilizer damping coefficient

K_{DP} pressure regulator piston damping coefficient

K_{DM} motor damping coefficient

K_{SD} stabilizer spring rate

K_{SP} pressure regulator loading spring rate

K_V pressure regulator variable orifice flow gain

L_D stabilizer inductance

M_D stabilizer mass

M_M motor piston mass

M_P pressure regulator piston mass

$\dot{m}$ mass discharge rate

P_L pressure regulator loading pressure

p_L perturbation in P_L

P_M motor pressure

p_M perturbation in P_M

P_R regulated pressure and relief valve pressure drop

p_R perturbation in P_R

P_S supply pressure

p_S perturbation in P_S

q_C compressibility flow perturbation

q_D stabilizer piston flow perturbation

Q_G flow generator flow rate

q_G perturbation in Q_G

Q_L load flow rate

q_L perturbation in Q_L

Q_M motor flow rate

q_M perturbation in Q_M

q_P pressure regulator piston flow perturbation

Q_V pressure regulator variable orifice flow rate

q_V perturbation in Q_V

R_G flow generator resistance

R_L load resistance

R_S system resistance

R_V pressure regulator variable orifice resistance

S Laplace operator

V volume in regulated pressure junction

v jet discharge velocity

V_M volume in motor

W pressure regulator variable orifice area lift gain

X_P pressure regulator piston position

x_D stabilizer piston position perturbation

x_M motor piston position perturbation

x_P perturbation in X_P

Z_L load impedance

Z_G flow generator impedance

Z_S pressure generator impedance

z_L perturbation in Z_L

α flow force area factor

β flow force spring rate factor

δ_P pressure regulator damping ratio

δ_A damping ratio of approximate quadratic

δ_D stabilizer damping ratio

δ_M motor damping ratio

δ_R pressure regulator with resistance load damping ratio

τ_D stabilizer time constant

τ_M motor time constant

τ_P product of loop gain and regulator time constant

τ_V pressure regulator time constant

τ_{DL} springless stabilizer time constant

ϕ angle between the discharge jet and the piston axis

θ gain margin ratio

ρ fluid weight per unit volume

ω_A undamped natural frequency of approximate quadratic

ω_D stabilizer undamped natural frequency

ω_M motor undamped natural frequency

ω_P pressure regulator undamped natural frequency

Appendix B

Derivation of Regulator Valve Flow Force Parameters

The force that results from the rate of change of momentum of a discharging jet is

$$F_Q = \dot{m} v \cos \phi \tag{B-1}$$

The relationship between the volumetric flow through the valve and the mass discharge rate is

$$\dot{m} = Q_V \frac{\rho}{g} \tag{B-2}$$

and the discharge velocity in the relief valve case is

$$v = C_V \sqrt{\frac{2gP_R}{\rho}} \tag{B-3}$$

Thus

$$F_Q = K_M Q_V \sqrt{P_R} \tag{B-4}$$

where

$$K_M = C_V \sqrt{\frac{2\rho}{g}} \cos \phi \tag{B-5}$$

From equation (B-4)

$$\frac{\partial F_Q}{\partial Q_V} = K_M \sqrt{P_R} = C_1 \tag{B-6}$$

$$\frac{\partial F_Q}{\partial P_R} = \frac{K_M Q_V}{2\sqrt{P_R}} = C_2 \tag{B-7}$$

The ratio of the two partial derivatives is

$$\frac{C_1}{C_2} = \frac{K_M\sqrt{P_R}}{\frac{K_M Q_V}{2\sqrt{P_R}}} = \frac{2P_R}{Q_V} = R_V \qquad \text{(B-8)}$$

In terms of perturbations

$$f_Q = C_1 q_V + C_2 p_R = C_1 q_V + \frac{C_1}{R_V} p_R \qquad \text{(B-9)}$$

Combining equations (B-9) and (3)

$$f_Q = C_1 K_V x_P + \frac{2C_1}{R_V} p_R \qquad \text{(B-10)}$$

The discharge velocity in the reducing valve case is

$$v = C_V\sqrt{\frac{2g(P_S - P_R)}{\rho}} \qquad \text{(B-11)}$$

and

$$F_Q = K_M Q_V\sqrt{P_S - P_R} \qquad \text{(B-12)}$$

From equation (B-12)

$$\frac{\partial F_Q}{\partial Q_V} = K_M\sqrt{P_S - P_R} = C_1 \qquad \text{(B-13)}$$

$$\frac{\partial F_Q}{\partial P_R} = -\frac{K_M Q_V}{2\sqrt{P_S - P_R}} = -C_2 \qquad \text{(B-14)}$$

$$\frac{\partial F_Q}{\partial P_S} = \frac{K_M Q_V}{2\sqrt{P_S - P_R}} = C_2 \qquad \text{(B-15)}$$

The ratio of the partial derivatives is

$$\frac{C_1}{C_2} = \frac{2(P_S - P_R)}{Q_V} = R_V \qquad \text{(B-16)}$$

In terms of perturbations

$$f_Q = C_1 q_V - C_2 p_R + C_2 p_S = C_1 q_V - \frac{C_1}{R_V} p_R + \frac{C_1}{R_V} p_S \qquad \text{(B-17)}$$

Combining equations (B-17) and (116)

$$f_Q = C_1\left(\frac{R_V - R_S}{R_V}\right) q_V - \frac{C_1}{R_V} p_R \qquad \text{(B-18)}$$

Substituting equation (117) in equation (B-18) yields

$$f_Q = \frac{C_1 K_V (R_V - Z_S)}{(R_V + Z_S)} x_P - \frac{2C_1}{(R_V + Z_S)} p_R \qquad \text{(B-19)}$$

The flow force is in the direction of valve closing in both the relief and the reducing valve configurations.

REFERENCES

1. Gold, Harold; and Otto, Edward W.: An Analytical and Experimental Study of the Transient Responses of a Pressure-Regulating Relief Valve in a Hydraulic Circuit. NACA TN 3102, 1954.
2. Merrit, Herbert E.: Hydraulic Control Systems. John Wiley and Sons, 1967.
3. Green, W. L.: The Stability of Poppet Relief Valves - A Summary. Hydraulic Pneumatic Power, vol. 18, no. 213, Sept. 1972, pp. 410-414.
4. Blackburn, John F.; Reethof, Gerhard; and Shearer, J. Lowen: Fluid Power Control. Technology Press of M.I.T. and John Wiley and Sons, 1960, sec. 17.3.
5. Keller, George R.: Hydraulic System Analysis. Industrial Publishing Co., 1969.
6. Ma, C. Y.: The Analysis and Design of Hydraulic Pressure - Reducing Valves. J. Eng. Ind., vol. 89, no. 2, May 1967, pp. 301-308.

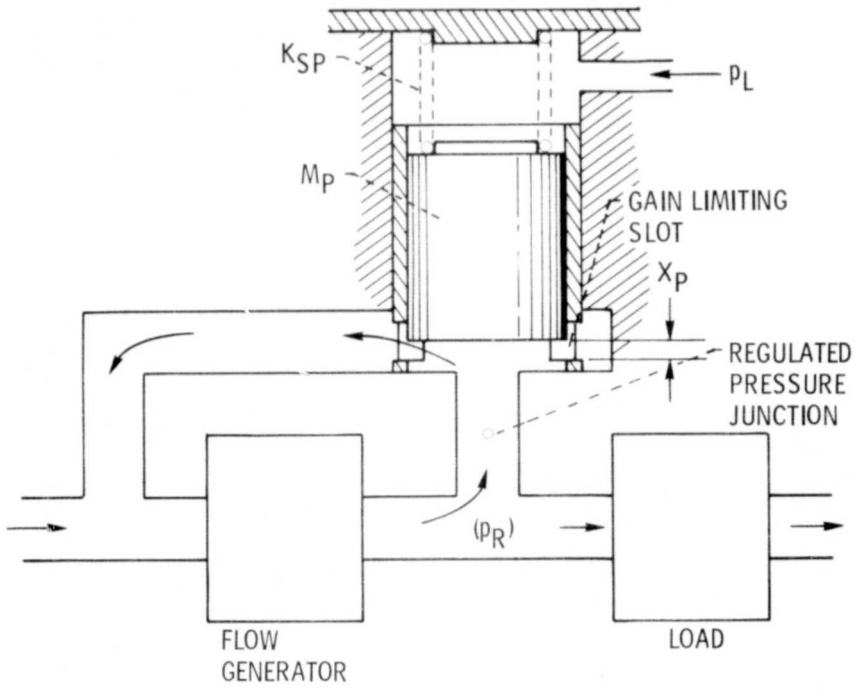

Figure 1. - Basic circuit and relief valve configuration.

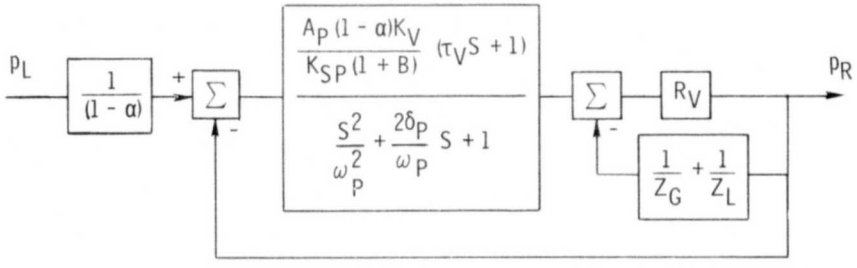

Figure 2. - Generalized block diagram of direct acting pressure regulators.

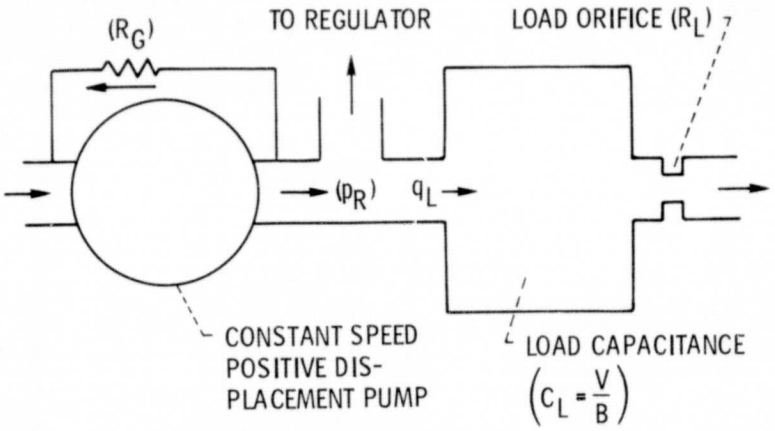

Figure 3. - Parallel capacitive plus resistive load.

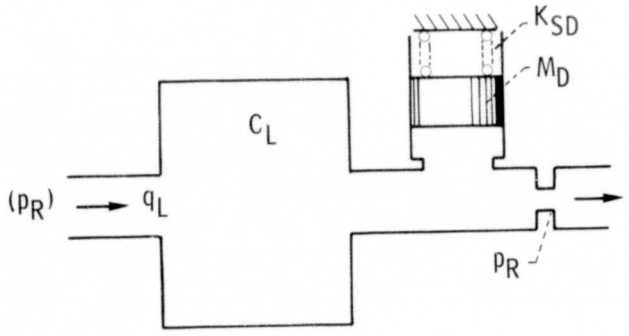

Figure 4. - Parallel capacitive plus resistive load and a tuned stabilizer.

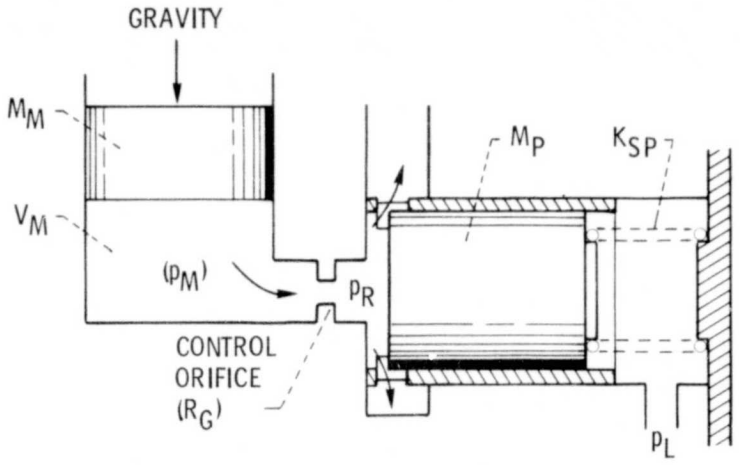

Figure 5. - Counterbalance valve circuit.

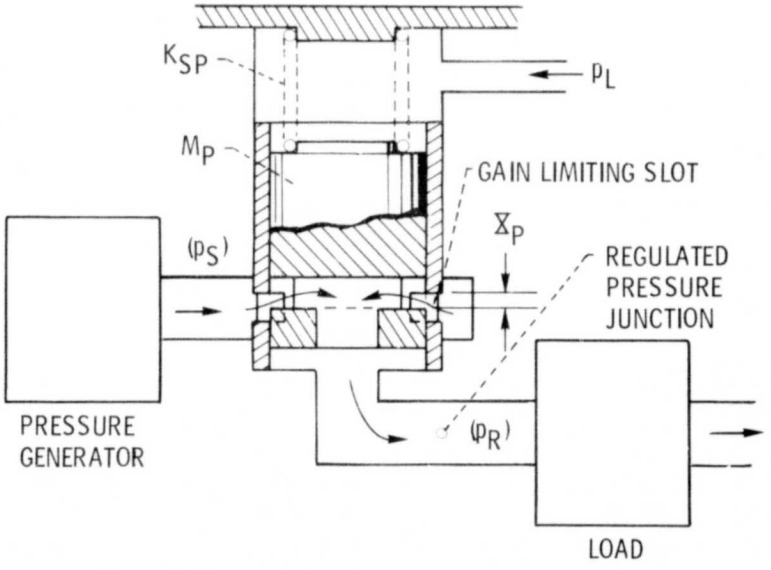

Figure 6. - Basic circuit and reducing valve configuration.

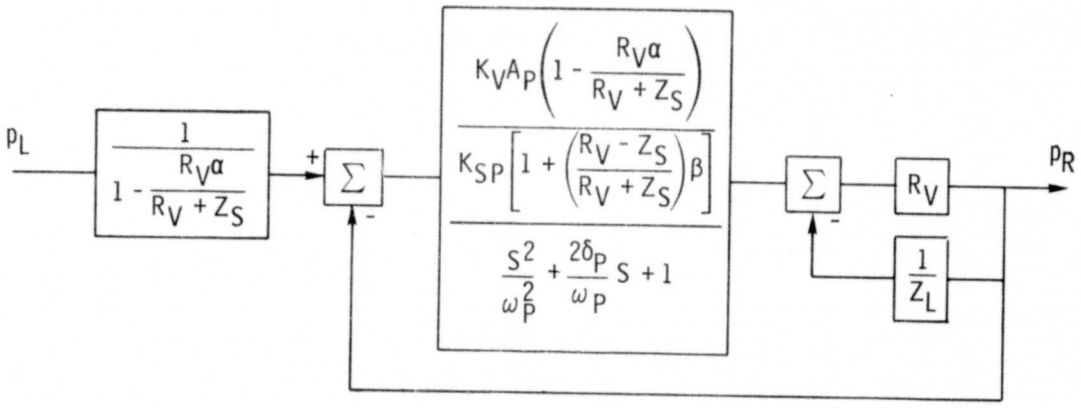

Figure 7. - Block diagram of direct acting pressure regulating reducing valves.

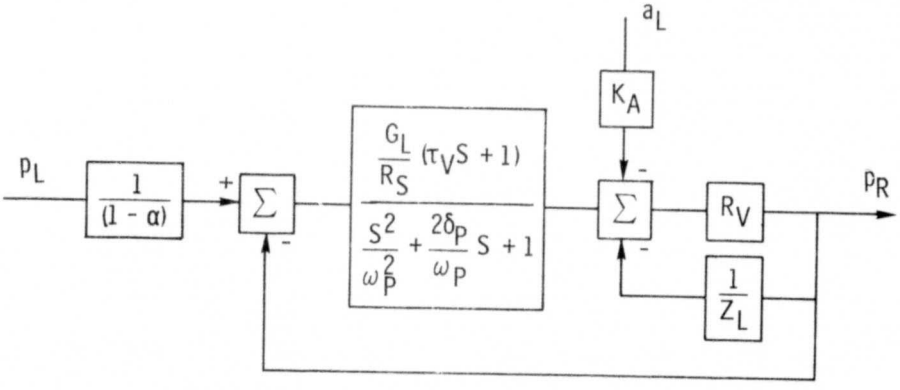

Figure 8. - Block diagram of direct acting pressure regulators subject to load orifice area disturbance.

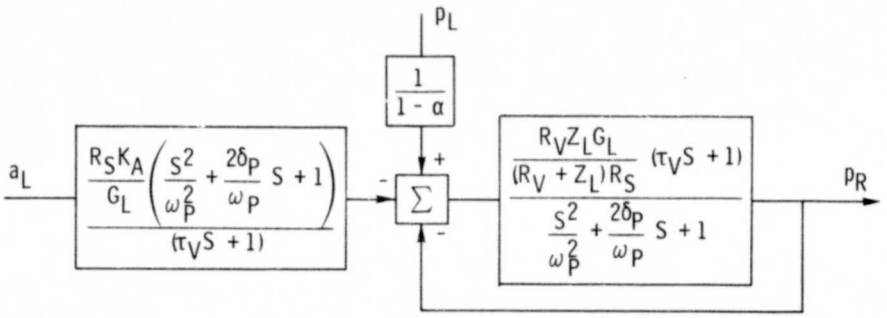

Figure 9. - Reduction of block diagram of figure 8.

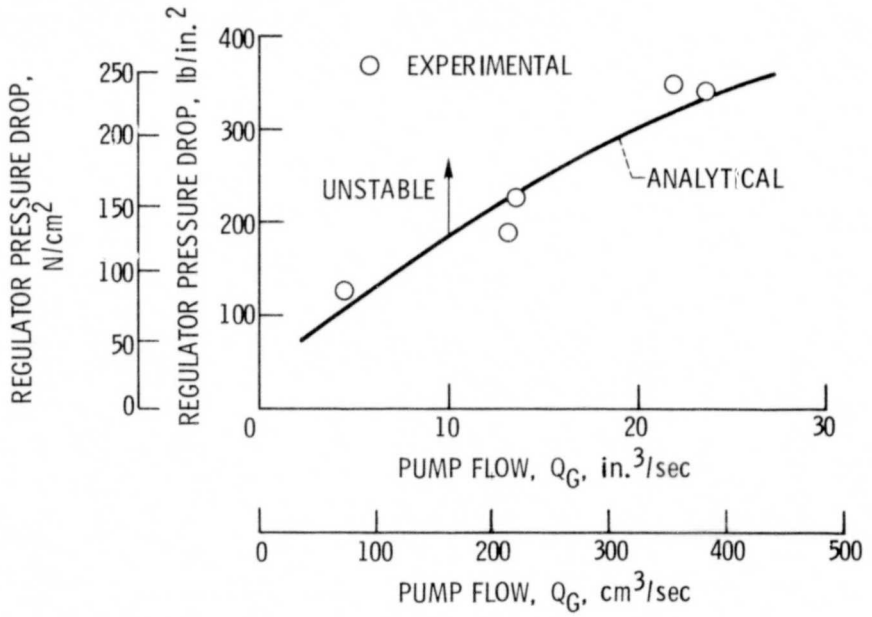

Figure 10. - Analytically and experimentally determined stability boundary. Relief valve pressure regulator, parallel capacitive plus resistive load.

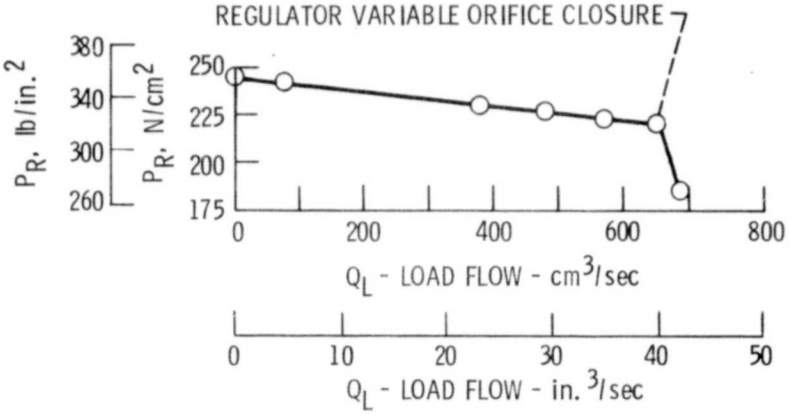

Figure 11. - Test pressure regulator droop calibration. Q_G = 43.3 in.^{3}/sec, V = 4.57 in.^{3}.

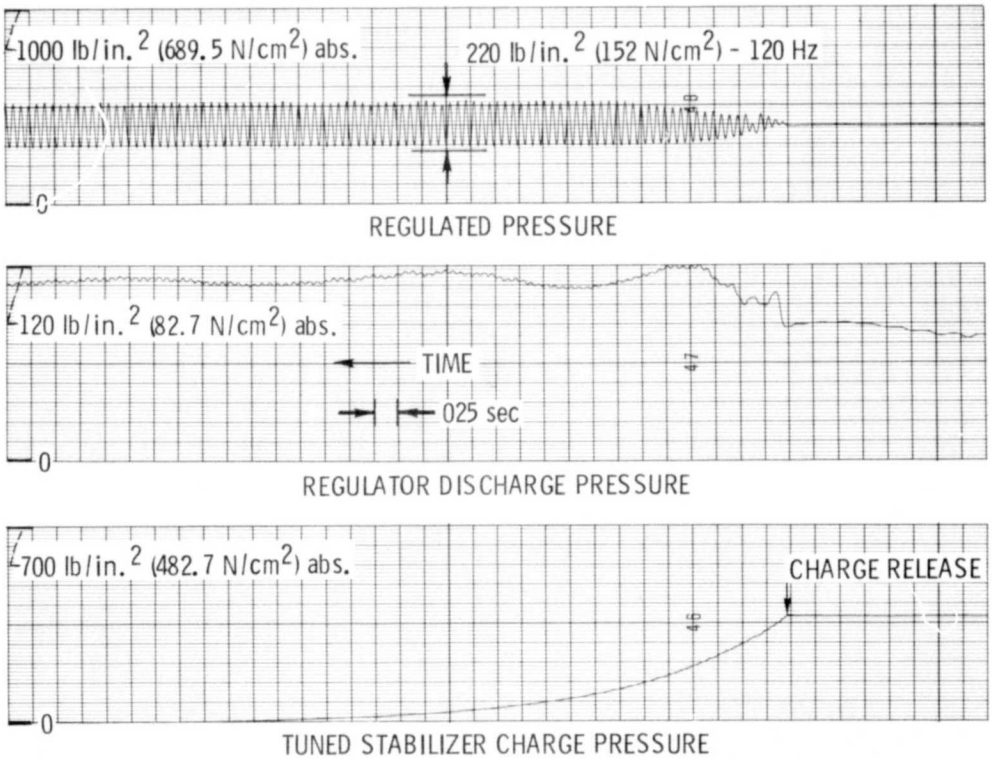

Figure 12. - Development of instability following release of tuned stabilizer charge air. Relief valve pressure regulator, parallel capacitive plus resistive load.

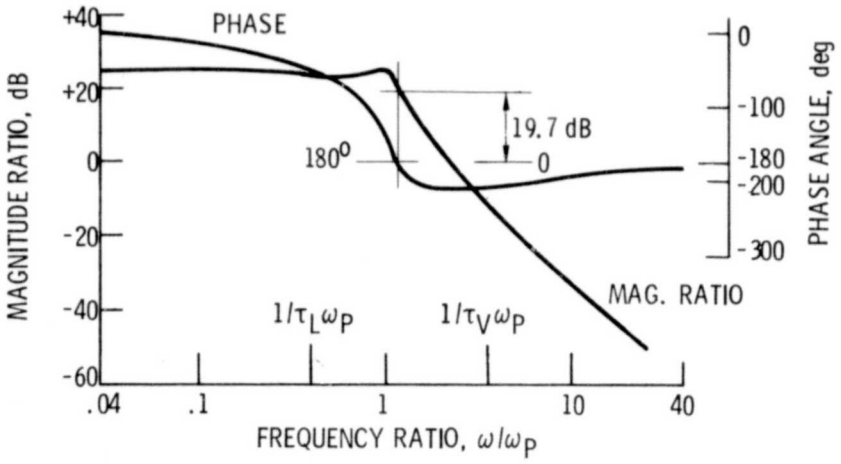

Figure 13. - Bode diagram of unstable pressure regulator. Parallel capacitive plus resistive load.

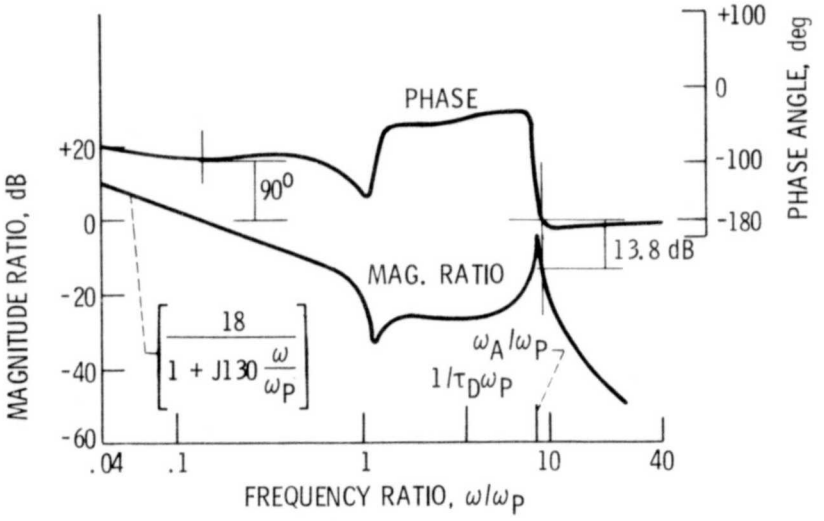

Figure 14. - Bode diagram of pressure regulator made stable by a tuned piston. Parallel capacitive plus resistive load.